Science of the Total Environment 409 (2011) 2443–2450

Contents lists available at ScienceDirect

Science of the Total Environment

journal homepage: www.elsevier.com/locate/scitotenv

Persistence of singly dispersed silver nanoparticles in natural freshwaters, synthetic seawater, and simulated estuarine waters

Stephanie L. Chinnapongse [1], Robert I. MacCuspie *, Vincent A. Hackley

Nanomechanical Properties Group, Material Measurement Laboratory, National Institute of Standards and Technology, 100 Bureau Dr, Gaithersburg, MD 20899-8520, USA

ARTICLE INFO

Article history:
Received 20 October 2010
Received in revised form 8 February 2011
Accepted 16 March 2011
Available online 9 April 2011

Keywords:
Silver nanoparticles
Nanoparticle stability
Dispersion
Environmental fate
Persistence

ABSTRACT

This investigation focuses on predicting the persistence of citrate-capped 20 nm AgNPs by measuring their colloidal stability in natural freshwaters and synthetic aquatic media. Ultraviolet–visible absorbance spectroscopy, dynamic light scattering, and atomic force microscopy were used to evaluate the colloidal stability of AgNPs in locally-obtained pond water, moderately hard reconstituted water alone or with natural organic matter (NOM), synthetic seawater, and also the individual chemicals most prevalent in seawater. Singly dispersed AgNPs in seawater and waters with greater than 20 mmol L^{-1} sodium chloride were unstable, with the optical absorbance approaching zero within the first ten hours of mixing. Agglomeration rates as a function of water chemistry and NOM are tested as a hypothesis to explain the rates of disappearance of singly dispersed AgNPs. Other samples, mostly those with lower salinity or NOM, maintained varying degrees of colloidal stability during time studies up to 48 h. This indicates likelihood that some AgNPs will be stable long enough in freshwater to successfully enter estuarine or marine systems. These results should enable a more efficient design of nanoEHS risk assessment experiments by predicting the aquatic or soil compartments at greatest potential risk for accumulation of and exposure to citrate capped 20 nm AgNPs.

Published by Elsevier B.V.

1. Introduction

The broad-spectrum biocidal properties of silver nanoparticles (AgNPs) are driving their use in a wide range of biomedical applications and consumer products, including medical devices such as catheters (Dair et al., 2010), and personal care products such as toothpaste and cosmetics (Wijnhoven et al., 2009). Potential applications include medical therapies for blocking HIV-1 transmission (Lara et al., 2010), surface plasmon resonance (SPR) based bioaffinity sensing (Frederix et al., 2003) and conductive inks used for printing circuit components (Perelaer et al., 2009). AgNPs are even being explored for point of use drinking water purification in third world countries (Oyanedel-Craver and Smith, 2008). While the quantity of AgNP enhanced products and devices in actual use today is difficult to assess, the broad interest in exploiting AgNP biocidal properties is indisputable (Sondi and Salopek-Sondi, 2004; Fauss, 2008; Sharma et al., 2009), including nomination for study by international bodies such as Europe's National Institute for Public Health and the Environment (RIVM) and the U.S. Food & Drug Administration (FDA) National Toxicology Program (Chemical Selection Working Group, 2006; Pronk et al., 2009). Additionally, regulatory bodies such as the U.S. Environmental Protection Agency (EPA) (2010) and FDA (2010) that are attempting to assess whether the nano form of bulk materials including silver presents new potential risks arising from nanoscale properties. Thus the potential for widespread use and subsequent life-cycle issues is of concern from an environmental, health and safety (EHS) perspective. Consequently, EHS impact and risk analysis of AgNPs has gained substantial momentum in recent years (Tolaymat et al., 2010), while public awareness has increased in parallel (Henig, 2007).

It remains unclear if the nanoscale form of silver presents a new EHS risk via novel modalities of the AgNPs themselves, or if AgNPs simply introduce a greater surface area of the bulk form of silver thereby increases the percentage of total atoms converted to soluble silver species (Ag^{+}) (Lok et al., 2007; Luoma, 2008; Badawy et al., 2010; Liu and Hurt, 2010; Liu et al., 2010), a legacy pollutant studied historically (Ribeiro Guevara et al., 2005; Figueroa et al., 2008). Recent studies have shown there is a risk that AgNPs could enter our waterways (Benn and Westerhoff, 2008; Blaser et al., 2008), yet questions remain as to the fate of such released AgNPs on various compartments of the environment—particularly aquatic ecosystems. The effects of AgNPs on aquatic environments have received some study to date. For example, AgNPs could be taken up by zebrafish embryos (Nallathamby et al., 2008) and can potentially be toxic at levels of 0.19 nmol L^{-1} of AgNPs or approximately 1 mg L^{-1} total Ag

* Corresponding author at: National Institute of Standards and Technology, 100 Bureau Dr, Mailstop 8520, Gaithersburg, MD 20899-8520, USA. Tel.: +1 301 975 6064; fax: +1 301 975 5334.
E-mail address: robert.maccuspie@nist.gov (R.I. MacCuspie).
[1] Current address: Georgia Institute of Technology, School of Civil and Environmental Engineering, 790 Atlantic Dr. Atlanta, GA 30332, USA.

0048-9697/$ – see front matter. Published by Elsevier B.V.
doi:10.1016/j.scitotenv.2011.03.020

(Lee et al., 2007), and AgNPs can inhibit photosynthesis in algae (Navarro et al., 2008), however the contributions from AgNPs alone or from dissolved Ag species is often unclear.

Questions remain regarding the stability of singly dispersed AgNPs under relevant conditions, and thus their persistence in the environment. For example, if AgNPs are colloidally unstable in natural freshwaters, they could potentially deposit in lake and river sediments; however, if AgNPs are stable in these aquatic systems they could continue to be transported into estuarine or even marine environments (Wen et al., 1997), where their stability could then change and potentially impact estuarine sediments (Bradford et al., 2009). Indeed, achieving reproducible dispersions for experiments and understanding aggregation phenomena has been identified as one of the greater challenges currently facing nanoEHS researchers (Wiesner et al., 2009). Understanding the colloidal stability of AgNP dispersions will enable better prediction of AgNP persistence in environmental waters and also benefit interpretation of toxicity studies.

The objective of this investigation is to apply high-througput screening methods for assessing the colloidal stability and agglomeration kinetics of AgNPs under conditions relevant to aquatic ecosystems, and to develop a robust method for predicting the persistence of AgNPs as singly dispersed entities. Since the colloidal stability will depend on the specific chemical environmentsthrough which the AgNPs transport, this paper will also briefly explore varying the concentrations of individual constituent chemicals of USEPA moderately hard reconstituted water (MHRW) and marine waters. Additionally, by providing well-characterized data sets as background to nanoEHS researchers, selection of the most relevant model systems is expedited during the design of future environmental risk assessment hypothesis-testing experiments employing singly dispersed AgNPs. Citrate-capped AgNPs approximately 20 nm in diameter were selected for this work based on the consensus recommendations of a workshop jointly organized by the National Institute of Standards and Technology (NIST) and the US Army Corp of Engineers held at Vicksburg, MS in April 2009.

2. Experimental[2]

Unless specified otherwise, all chemicals were purchased from Sigma Aldrich (St. Louis, MO, USA) of the highest purity available and used as received without further purification. All salt solutions were prepared using 18.2 MΩ cm deionized (DI) water obtained from an Aqua Solutions (Jasper, GA, USA) Type I biological grade water purification system outfitted with an ultraviolet lamp to oxidize residual organics and a low relative molecular mass cut-off (MWCO) membrane.

2.1. Synthesis of AgNPs

AgNPs were synthesized via reduction of silver nitrate ($AgNO_3$) by sodium borohydride ($NaBH_4$) in the presence of sodium citrate, reported elsewhere (MacCuspie, 2011), and described in detail in the supplemental information; the AgNPs will be referred to as nominally 20 nm in diameter. The AgNPs were concentrated to approximately 1 mg mL^{-1} then purified by washing with five volumes of DI water using stirred cell ultrafiltration with a 10,000 Da relative MWCO regenerated cellulose membrane (Millipore, Billerica, MA). Initial physico-chemical characterization (Supporting Info) was performed after concentration. All AgNPs were used within eight weeks of synthesis.

2.2. Sampling of natural fresh waters

Three samples of natural fresh waters were collected from the NIST Gaithersburg, MD campus. A sample of approximately 500 mL of water was obtained from the western shore of the northern pond (PW N), southern pond (PW S), and creek connecting the two ponds (PW M), located near 39.13 °N, 77.21 °W. A clean wide-mouthed 500 mL polyethylene bottle was slowly immersed in a horizontal position approximately 2 ft from the edge of the shore with care taken to not create bubbles or strong mixing currents from water flowing into the container. The container was slowly lowered to the bottom to avoid disturbing bottom sediments, turned vertically, then lifted up out of the water and capped. Samples were collected on June 26, 2009 between 11:00 am and 11:30 am, and stored at room temperature until use. PW stocks were shaken before use to resuspend any sediment that had settled during storage. The PW samples used in these experiments had noticeable cloudiness in the samples, suggesting the presence of significant amounts of natural organic matter (NOM). Algae were more prevalent in the pond from which South PW was taken based on visual observation.

2.3. AgNP dispersion preparation

Dispersion samples were prepared by adding 10 μL of AgNPs to 990 μL of the media (approximate final AgNP concentration 1.4×10^{-10} mol L^{-1}). AgNPs were added immediately before measurements, shaken by hand to mix the samples, and typically less than 2 min elapsed between the mixing of samples and the start of a measurement. Media included the three PWs, or synthetic seawater (SW) conforming to ASTM International standard D1141 (Ricca Chemical, Arlington, TX). For salt media, including sodium chloride (NaCl), magnesium chloride ($MgCl_2$), sodium bicarbonate ($NaHCO_3$), sodium sulfate (Na_2SO_4) and calcium chloride ($CaCl_2$), an appropriate aliquot of 100 mmol L^{-1} stock salt solution was added to a volume of DI water such that the salt media volume was 990 μL before addition of the AgNPs and the desired concentration of salt (e.g., 10 mmol L^{-1}) was correct in the final 1.00 mL dispersion. Moderately Hard Reconstituted Water (MHW) was prepared according to EPA guidelines (USEPA, 2002). Stock solutions of Suwannee River Standard I and Standard II (International Humic Substances Society, St. Paul, MN), which will be referred to as NOM I and NOM II, were prepared in DI water at 1.00 mg mL^{-1}, and 10 μL were added to 890 μL of either DI water or MHW before addition of 100 μL of diluted AgNPs (0.06 mg mL^{-1}), making the final NOM concentration 10.0 μg mL^{-1} or 10.0 parts per million.

2.4. Dynamic light scattering (DLS)

DLS measurements were performed in accordance with established standard protocol NIST & National Cancer Institute Nanotechnology Characterization Laboratory (NIST-NCL) PCC-1 Protocol (Hackley and Clogston, 2007), using a Malvern Instruments (Westborough, MA) Zetasizer Nano in 173° backscatter mode, with Z-average values reported as the mean of no less than five consecutive measurements plus or minus one standard deviation about the mean. Disposable semi-micro cuvettes were cleaned with filtered compressed air immediately before use. The instrument was equipped with a temperature controller set at (20.0 ± 0.1) °C for all experiments.

[2] Certain trade names and company products are mentioned in the text or identified in illustrations in order to specify adequately the experimental procedure and equipment used. In no case does such identification imply recommendation or endorsement by National Institute of Standards and Technology, nor does it imply that the products are necessarily the best available for the purpose.

2.5. Ultraviolet–visible (UV–vis) spectroscopy

A split-beam spectrometer equipped with a water-jacketed 8 + 8 cell changer for matched pairing of reference cuvettes to sample cuvettes (ultraviolet-transparent disposable semi-microcuvettes with a 1 cm pathlength) was employed; all experiments were performed at (20.0 ± 0.2) °C. Full spectra of AgNPs in various media were collected every hour, to ensure that the peak absorbance wavelength (λ_{max}) was stable (Link and El-Sayed, 1999; Malinsky et al., 2001).

2.6. Atomic force microscopy

NIST–NCL PCC-6 protocol was followed (Grobelny et al., 2009). AFM measurements were performed in intermittent contact or tapping mode using a closed-loop scanner. Cantilevers from the same production lot with a reported spring constant of 7.4 N m^{-1}, and a reported tip radius of curvature of approximately 8 nm were used.

3. Results

To observe the persistence of singly dispersed citrate capped 20 nm AgNPs in environmental waters, AgNPs were dispersed in the three natural freshwater samples. The SPR absorbance at λ_{max} of single AgNPs remaining in solution over time is summarized in Fig. 1a, showing decreased absorbance for all PWs and SW. Examination of the full spectra over time (also referred to as waterfall plots, and reported in the SI) reveals that peaks at longer wavelengths appear over time. For PW N (Fig. 1b), the red-shift in maximum wavelength of the agglomerate peak combined with the steady absorbance over time suggests stable agglomerates were forming and increasing in size. For PW M (Fig. 1c), the very broad absorbance at longer wavelengths suggests much larger agglomerates, that are much more likely to settle out of the beampath quickly during the 48 h of observation. For PW S (Fig. 1d), a greater red-shift in the peak indicates larger increases in agglomerate size, although the decreasing absorbance suggests these agglomerates are only transiently stable. On visual inspection after the experiment, a thin layer of dark solid material was observed on the bottom of the cuvette below the optical path.

The kinetics of the stability of single AgNPs in simulated estuarine waters was also evaluated. Mixtures with varying percentages of PW and SW were also analyzed by UV–vis spectroscopy for 36 h, with the absorbance at λ_{max} over time plotted in Fig. 2a (see SI for full spectra). AgNPs in waters containing greater volume percentages of SW were observed to have a more rapid decrease in absorbance at λ_{max} (Fig. 2a). The greatest instability observed was single AgNPs in SW, with less than 20% of the AgNPs remaining after just 1 h and no detectable absorbance after 10 h.

The absorbance data were fit to a pseudo-first order kinetics model (Templeton et al., 1998), originally developed to model the reactivity of stericly hindered gold nanoparticles. The model, discussed in detail later, uses $y = b + a\ \exp(-k_{obs}t)$, where y is the absorbance, b is defined as the persistent fraction of singly-dispersed AgNPs, a is a fitting parameter, k_{obs} is the observed rate constant of single AgNP disappearance (through any mechanism), and t is time. The fitted parameters b and k_{obs} are plotted in Fig. 2b as a function of percentage of PW S in the simulated estuarine water. Low persistent fractions after 36 h were found for mixtures with 50% or less PW S.

DLS data in Fig. 3a show increasing sizes of structures suspended in various solutions over time, including SW, MHW, MHW + NOM I and the three PW samples. The notable exceptions are PW N and MHW + NOM II, in which significant colloidal stability was observed. This is further suggested by the broadening of the SPR λ_{max} peak in PW N compared to DI water (see Figure SI-4). Also interesting was the behavior of PW M and MHW + NOM I following nearly identical DLS size increases. A DI water control had constant absorbance (Figure SI-29) and DLS size (data not shown). AFM of AgNPs in DI water

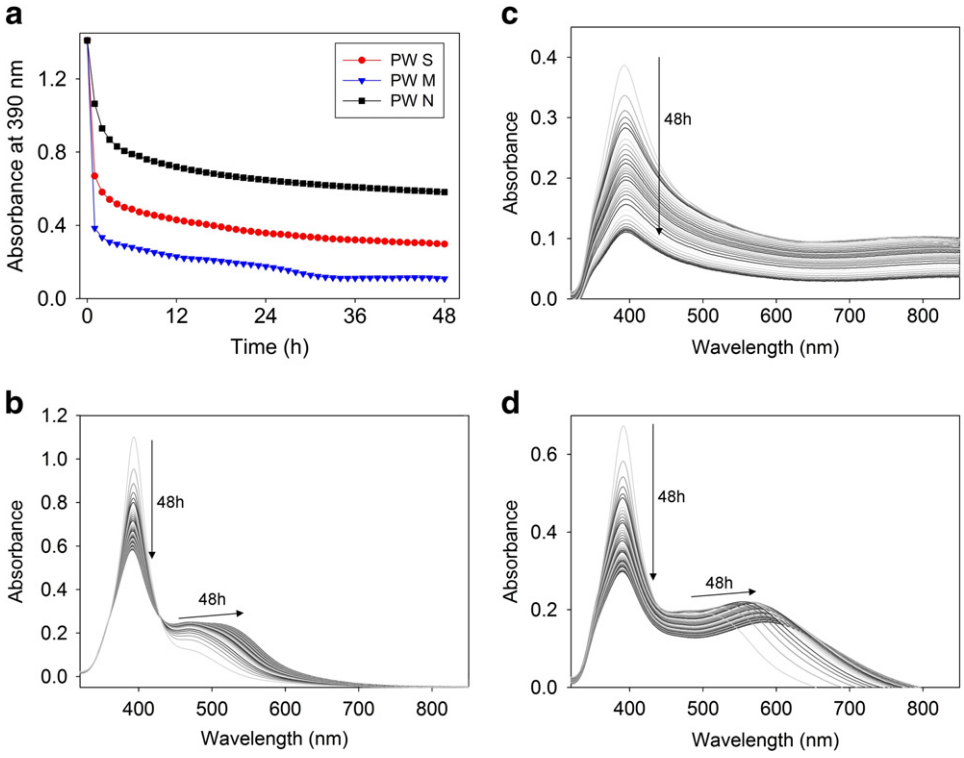

Fig. 1. (a) Colloidal stability of citrate-capped AgNPs measured by UV–vis absorbance over time for three natural freshwaters. Data points are the mean of two experiments, with symbols drawn larger than the difference, lines are to guide the eye. Waterfall-style plots of absorbance spectra collected over time of citrate capped AgNPs in the three natural freshwaters collected (b) PW N, (c) PW M, and (d) PW S.

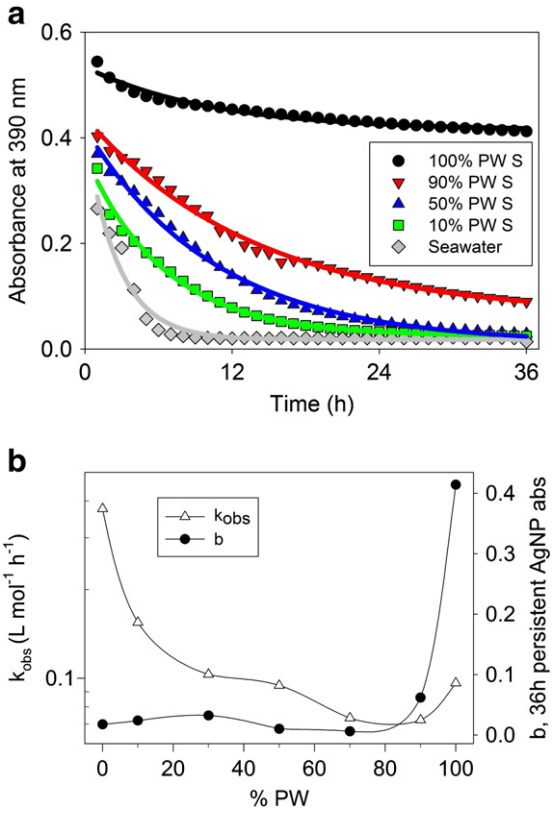

Fig. 2. (a) Colloidal stability of citrate capped AgNPs measured by UV–vis absorbance over time for mixtures of varying ratios of PW S and SW; lines are fits from pseudo-first order kinetics model. (b) Plot of fitted kinetics parameters, observed rate constant, k_{obs}, and fraction of persistent singly dispersed AgNPs after 36 h, *b*, as a function of freshwater to seawater ratio.

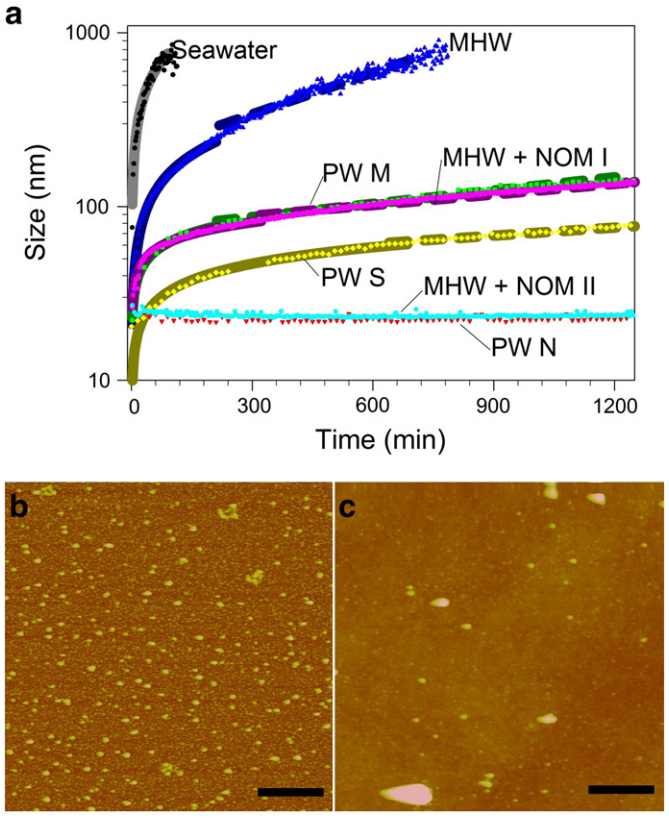

Fig. 3. (a) DLS data over time for citrate capped AgNPs in various environmentally relevant waters; points represent data, solid lines represent DLCA model fits, and dashed lines represent RLCA model fits. AFM images of citrate capped AgNPs diluted with (b) DI water and (c) moderately hard water. Scale bars are 400 nm.

(Fig. 3b) revealed only singly dispersed AgNPs, while AgNPs dispersed in MHW showed signs of agglomeration (Fig. 3c) and increasing polydispersity, in agreement with the DLS data.

The stability of single AgNPs in various concentrations of single salts including $CaCl_2$, $MgCl_2$, NaCl, $NaHCO_3$, and Na_2SO_4 (representing the major components of synthetic seawater) were analyzed by UV–vis absorbance over time, and also fit to pseudo-first order kinetics. The fitted parameters of k_{obs} and *b* were plotted as a function of the Debye Length (discussed later) in Fig. 4a and b, respectively. The concentration ranges for which rapid agglomeration (defined for this report as greater than 80% absorbance loss in 1 h) began to occur was found to be above 50 mmol L^{-1} Na_2SO_4, between (20 and 50) mmol L^{-1} NaCl, near 10 mmol L^{-1} $NaHCO_3$, below 1.0 mmol L^{-1} $MgCl_2$, and between (0.1 and 1.0) mmol L^{-1} $CaCl_2$.

4. Discussion

4.1. AgNP persistence in natural waters

This paper will use a working definition of persistence such that only untransformed singly dispersed AgNPs with colloidal stability will be persistent in the environment. This is also relevant to nanoEHS experiments dosing well-characterized AgNPs for hypothesis testing.

To predict the persistence of singly dispersed AgNPs in natural waters, the temporal stability of AgNPs in various media was measured primarily using UV–vis absorbance, with spot-checks by DLS and AFM. UV–vis is especially attractive when the primary concern is the concentration of singly dispersed AgNPs remaining in the solution of interest. The validation for using primarily UV–vis as a rapid, low-cost, pre-screening tool measuring the concentration of single, well-dispersed AgNPs in a solution is described elsewhere (MacCuspie et al., 2011a; MacCuspie et al., 2011b).

To simulate the potential fate of AgNPs released into an aquatic environment, three natural freshwaters or PWs were used. The fraction of single AgNPs that were stable for 48 h varied by PW sampling location, as observed by UV–vis (Fig. 1a). PW N, S and M displayed decreasing stable fractions of singly dispersed AgNPs, respectively. In all cases, an initially rapid rate of singly dispersed AgNP disappearance during the first ten hours transitioned to a much slower rate of disappearance at later times. These AgNPs that remained suspended at 48 h reveal that each freshwater sample has a different capacity for stabilizing the AgNPs against agglomeration, despite tight geographical clustering of the samples.

To model the change in AgNP stability as NPs move from freshwater through estuarine bodies into ocean water, PW S was mixed with various quantities of SW. To compare the rates of AgNP disappearance over tens of hours, pseudo-first order kinetics was assumed for the instability. As absorbance was only measured once per hour, the initial rapid diffusion limited aggregation, which follows second order kinetics, can be expected to be over half completed by the end of the first hour based on reports of AgNPs in biological fluids. Once aggregates have grown substantially, and their diffusion rate is much slower than the single particles, first order kinetics with respect to the singly dispersed AgNPs may occur. Additionally, previous reports of kinetics on reactions that dissolve gold NPs use pseudo-first order kinetics. Here, the assumption is made that chemical reactions would act upon singly dispersed AgNPs, and if they depend upon the concentration of a second reactant it would remain in constant concentration relative to the AgNPs (*e.g.*, there is an infinite sink of dissolved oxygen from the atmosphere).

As k_{obs} is the fitted observed rate constant of single AgNP consumption, k_{obs} is the sum of all single AgNP disappearance kinetics

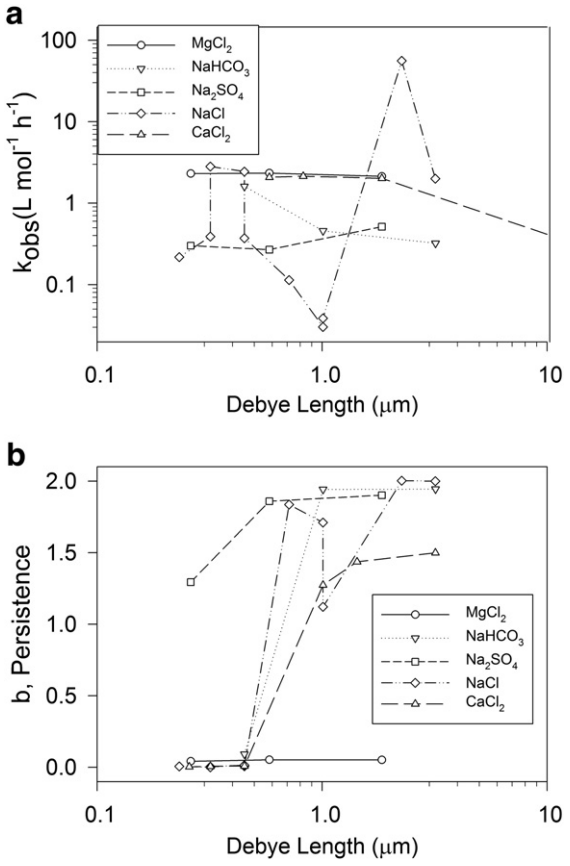

Fig. 4. Colloidal stability of AgNPs in various concentration of electrolytes measured by UV–vis absorbance over time with pseudo-first order kinetics fits of (a) k_{obs}, the rate of single AgNP disappearance, and (b) b, the persistent absorbance of single AgNPs, plotted as a function of κ^{-1}, Debye length. The time end-point for the kinetics experiments are 96 h for NaCl, 24 h for $CaCl_2$, and 15 h for $MgCl_2$, Na_2SO_4, and $NaHCO_3$. See Figures SI-15 to SI-33 for full spectra over time.

including k_{agg} from all colloidal instabilities and sedimentation out of the beam path by those agglomerates, k_{rxn} from all chemical reaction kinetics which could include both dissolution of the AgNPs into various silver polychloride anion complexes or surface chemistry reactions such as oxidation that could eliminate the SPR, and k_{other} which will include all contributions that are not discussed, such as adhesion to cuvette walls or sedimentation of singly dispersed AgNPs, which are assumed to be negligible on the up to 96 h timescales of this work.

By plotting the fitted kinetics parameters as a function of the percentage of PW (Fig. 2b), a trend was revealed that shows the fastest observed instability kinetics occurred above 90% SW by volume. Also, the addition of just 10% SW to PW S led to a 60% lower SPR peak absorbance after just 1 h compared to the PW S alone. Increasing the SW content above 10% by volume caused only slight changes in k_{obs}. This led to the hypotheses that the dominant mechanism of removal of singly dispersed AgNPs is colloidal instability (*i.e.*, $k_{agg} >> k_{rxn}$), the rate is accelerated through charge screening induced agglomeration, and the rate is slowed by the presence of NOM.

4.2. Potential mechanisms of singly dispersed AgNP instability

Classical colloidal chemistry concepts were employed to test the hypotheses above. By examining different scenarios where agglomeration would be expected to occur and measuring the rates of AgNP persistence in these laboratory waters, comparisons could be made to the more complex natural water samples. For example, charge screening due to the presence of electrolytes or divalent cations should yield similar singly dispersed AgNP disappearance kinetics if $k_{agg} >> k_{rxn}$. Similary, by the addition of steric stability through surface adsorption of NOM, a decrease in k_{agg} should be observed.

4.2.1. Role of electrolytes

The most prevalent electrolyte components of SW were tested individually in a series of concentrations bracketing the natural concentrations. The electrolytes selected were $CaCl_2$, $MgCl_2$, NaCl, Na_2SO_4, and $NaHCO_3$. The concentration ranges where rapid agglomeration began to occur were found to be below the concentration of NaCl in SW, suggesting the large NaCl concentration alone could be the source of the rapid instability, as would be predicted by DLVO theory.

In the case of MHW, the concentration of potassium chloride (KCl) is 54 μmol L^{-1}, too low to induce rapid aggregation by DLVO theory and suggesting that other constituents are the root cause of the instability. Indeed, a previous report shows that AgNPs in 10 mmol L^{-1} of either LiCl, NaCl or KCl all agglomerate slowly, with less than 10% loss of λ_{max} absorbance during 72 h (MacCuspie, 2011). The AgNPs were stable in 1.00 mmol L^{-1} $NaHCO_3$ (Figure SI-21), ruling out $NaHCO_3$ as the primary source of instability as its concentration in MHW is 1.143 mmol L^{-1}. Although stable in 0.1 mmol L^{-1} $CaCl_2$ (Figure SI-31), the AgNPs were rapidly unstable in 1.00 mmol L^{-1} $CaCl_2$ or $MgCl_2$ (Figures SI-32 and SI-15, respectively). As the combined concentration of divalent cations in MHW is 0.846 mmol L^{-1}, this data confirms that the concentration of divalent cations is the most important parameter of water hardness in terms of predicting the persistence of singly dispersed AgNPs.

Modern applications of DLVO theory, include more terms than simply the sum of the van der Waals attractive and electrostatic repulsive forces to describe the more complex nature of nanoparticles in relevant media, such as compressible coatings on the surfaces of AgNPs (Stebounova et al., 2011). If the only source of AgNP instability is from agglomeration due to charge screening, then the fitted k_{obs} from the UV–vis absorbance data will be only a function of k_{agg}. The electrostatic repulsive forces are dependent upon the Debye length, κ^{-1}, or charge screening length. If the electrolyte composition and concentration of a solution is known, κ^{-1} can be calculated analytically using the Debye–Hückel equation. When the k_{obs} results are plotted as a function of κ^{-1}(Fig. 4a), they did not converge as would be expected if the only instability were arising from charge screening. This is in contrast to the persistent fraction, b (Fig. 4b), where a transition of b from large values to near-zero values occurred across a similar κ^{-1} range, irrespective of the electrolyte for the single electrolyte waters. This lack of convergence by k_{obs} provides clues as to what other mechanisms may affect AgNP persistence. It is possible that other mechanisms beyond colloidal instability, such as chemical reactions of the Ag(0) in the AgNPs that eliminate the SPR, could also be contributing to the disappearance of singly dispersed AgNPs. In other words, terms beyond k_{agg} are contributing to k_{obs}, and these terms are of similar magnitude as k_{agg}. Nevertheless, the impact on the persistence of AgNPs in environmental waters is clear, that increasing water hardness or salinity will lead to rapid agglomeration and sedimentation out of the water column without some other stabilizing forces, such as adsorbed NOM coatings.

4.2.2. Role of NOM on AgNP persistence

In evaluations of the results from the natural freshwaters, the effects of NOM on AgNP persistence must be considered. NOM is ubiquitous in aquatic systems and can serve to either augment or reduce NP stability, depending on the nature of the organic molecules. For example, humic substances have been reported to increase stability of carbon nanotube dispersions (Chappell et al., 2009). As it has been reported that NPs dynamically sorb and desorb proteins as the biological matrix they are exposed to changes (Walczyk et al.,

2010), under a hypothesis that NOM will adsorb to the surface of the AgNPs, it would follow that the properties of the AgNPs would thus transform. However, the chemical composition of natural freshwaters (including type and concentration of NOM) is widely variable given different locations or even recent rainfall patterns. Additionally, quantitatively measuring the surface molecular composition of nanoparticles remains very challenging beyond well-defined systems with only one or two known molecules (Jackson et al., 2006; Tsai et al., 2010; Geronimo and MacCuspie, 2011; Tsai et al., 2011).

A series of well-defined systems for study of the role of specific components in NOM on the colloidal stability of the AgNPs were prepared. This series included MHW alone and mixed with Suwannee River humic substance standards at concentrations less than half of typical Suwannee River conditions (Averett et al., 1994), in addition to pure SW and the aforementioned PW samples.

Since the UV–vis data only provides the rate of disappearance of single AgNPs, DLS was selected to observe if agglomerates were forming and measure their size over time. While red-shifted broad absorbance does indicate the presence of agglomerates, it is worth noting that the absence of absorbance at red-shifted wavelengths does not automatically assure the absence of agglomerates, as they may settle below the spectrometer beam path (see SI for more discussion on UV–vis absorbance). This was evidenced by the sediment on the bottom of all SW + PW cuvettes, noted during visual inspection after removal from the UV–vis spectrometer.

Fig. 3a shows data points as symbols, with diffusion limited colloidal aggregation (DLCA) model fits shown as solid lines. The DLS data revealed that agglomerates were present and growing in size over time in most waters. The exceptions were AgNPs in PW N and MHW + NOM II, which showed no change in diameter within the uncertainty of the DLS measurement for greater than 48 h of observation. Note, while data collection continued beyond the points plotted in Fig. 3a, the size of the agglomerates approached the limits of the DLS technique (diameters of approximately 1 μm), and was determined to be too ambiguous to be meaningful.

DLCA growth kinetics follow a relationship in which the diameter of the agglomerate is proportional to agglomeration time (*i.e.* the time after mixing) raised to the power α, where α is the reciprocal of the fractal dimension of the agglomerate. For DLCA of electrostatically stabilized gold, silica, or polystyrene nanoparticles, α was experimentally previously determined to be in the range of 0.53 to 0.56 (Lin et al., 1989), and α values of 0.52 and 0.53 were observed here for SW and MHW, respectively.

However, PW M, PW S, and MHW + NOM I showed initial DLCA-like periods (*i.e.* the DLCA power-law model could be fit to the DLS data, but with α values between 0.22 and 0.31), suggesting that some factor was retarding the truly diffusion limited kinetics observed in the SW case. Measuring the size of agglomerates hundreds of nanometers in size over many hours might produce an artifact of apparent "slower" growth kinetics at longer times, since particles start to sediment faster as they grow in size.

In PW M, PW S and MHW + NOM I, the early rapid-growth period eventually gave way to a period of slower DLS diameter growth. This is consistent with NOM molecules sorbing onto the surface of the AgNPs and the agglomerates, providing increased steric repulsive energy. This is in agreement with a recent report on forming stable agglomerates, where quenching the agglomeration process with concentrated excess protein immediately halts agglomerate size growth (Zook et al., 2011). The lower concentration of NOM in this study (by orders of magnitude) likely accounts for the residual slow growth rate of the agglomerates.

If a transition from DLCA to reaction limited colloidal aggregation (RLCA) is taking place at this point, due to an energy barrier to aggregation created by the adsorption of a NOM layer, the log of the agglomerate diameter is proportional to the time after mixing. Indeed, in Fig. 3a the relationship between DLS diameter and time is linear on a semi-logarithmic plot at later times, with dashed lines representing a RLCA model fit of diameter being proportional to $\exp(t_a/t_0)$, where t_a is the agglomeration time, or time after mixing, and t_0 is the agglomeration time constant.

Differences in agglomeration time constant across water type were revealed. The two types of NOM, when in MHW, provided either complete stability (II, Humic) or a very slow t_0 (I, Fulvic) compared to MHW alone. Since in order for a molecule to increase the colloidal stability of a AgNP it must be associated with the surface of the AgNP, this data also suggests that the humic standard may have a stronger binding affinity towards the AgNP surface.

Interestingly, MHW + NOM I and MHW + NOM II provided time constant "boundaries" that the three PW samples either aligned with or fell between. PW M had the largest agglomerates by DLS and also had the greatest decrease in λ_{max} absorbance (Fig. 1a). Additionally, across the three natural waters, SW, and MHW, the rate of increase in agglomerate size followed the same trend as the rate of decrease in λ_{max} absorbance, indicating that k_{agg} must be significantly contributing to k_{obs}.

Yet these results do not explain the persistent fraction. It is possible that due to the large size of some NOM molecules that several individual AgNPs adsorb to the surface of the NOM with sufficient spacing that the SPR of the AgNPs cannot couple, therefore they continue to provide absorbance at λ_{max}. Yet, because the NOM-multi-AgNP agglomerate is behaving hydrodynamically as one large entity, the DLS size continues to grow as additional AgNPs continue to join the agglomerate.

These results imply that a significant fraction of the initially singly-dispersed AgNPs will agglomerate and sediment to the soils of freshwater environments near their point of introduction. Another fraction of the AgNPs will remain persistent enough in freshwaters to be transported into estuarine waters, putting those aquatic compartments at risk to single AgNPs. These results could potentially help explain previous observations of the presence of colloidal silver in Texas estuaries reported in the 1990s (defined then as 100 nm to 450 nm), years before the recent surge in AgNP consumer products (Wen et al., 1997).

5. Conclusion

These stability studies on AgNPs in pond water and SW make it clear that the potential toxicity of AgNPs will likely affect both freshwater and ocean environments. Citrate stabilized AgNPs nominally 20 nm in diameter partially agglomerated in the three PW samples tested, with varying fractions of AgNPs remaining in solution at equilibrium. UV–vis, DLS, and AFM indicated that even after agglomerates had formed, stable AgNPs remained that could then migrate into estuarine or SW. AgNPs were least stable in SW, losing electrostatic colloidal stabilization rapidly due to charge screening by greater NaCl concentrations and the presence of divalent cations. In mixtures of pond water and SW, the NOM likely provided some limited colloidal stabilization, whereas the kinetics of AgNP disappearance increased as the fraction of SW increased.

As UV–vis and AFM data indicated that some fraction of AgNPs retained colloidal stability in all pond water samples, it is a reasonable assumption that a fraction of the AgNPs that enter our waterways will reach estuarine systems in the form of single AgNPs, then experience more rapid agglomeration and sedimentation rates with increasing salinity with very few if any AgNPs reaching marine environments. These results could be applied to potentially create a map with a "zone of dispersion" and "zone of agglomeration" based on maps of the salinity of freshwaters and estuarine waters combined with typical seasonal water flow rates (Lung and Nice, 2007; Zou et al., 2009). Using the paradigm of hazard × exposure equals risk, if the use of AgNPs by the consumer products industry continues to grow at its current rate then the risk could increase, even though the potential

hazards of AgNPs are unclear and may in fact be low if designed appropriately (Harper et al., 2008). Future work should explore the kinetic effects of varying pH (Elzey and Grassian, 2010), dissolved oxygen, temperature, and specific constituents of NOM (Akaighe et al., 2011), all of which are also likely to play important roles in the colloidal and chemical stability of AgNPs in environmental waters.

These results are also significant because in addition to stable agglomerates, the stabilized AgNP form itself (beyond dissolution into Ag^{+}) must be studied for novel nanoEHS hazard. The data presented here indicates that AgNPs have the potential to impact both estuarine and freshwater sediments and associated aquatic vegetation and organisms, suggesting a continued need for development of a broad array of model systems for nanoEHS risk assessment.

Acknowledgements

S.L.C. was supported in part by the National Science Foundation's Research Experience for Undergraduates (REU) program, Division of Materials Research, and through the NIST Summer Undergraduate Research Fellowship (SURF) program.

Appendix A. Supplementary data

Supplementary data to this article can be found online at doi:10.1016/j.scitotenv.2011.03.020.

References

Akaighe N, MacCuspie RI, Navarro D, Aga D, Banerjee S, Sohn M, Sharma VK. Humic Acid-Mediated Silver Nanoparticle Formation Under Environmentally Relevant Conditions. Environ Sci Technol 2011, doi:10.1021/es103946g ASAP.

Averett RC, Leenheer JA, McKnight DM, Thorn KA. Humic substances in the Suwannee River, Georgia: interactions, properties, and proposed structures. USGS Water-Supply Paper; 1994. p. 2373.

Badawy AME, Luxton TP, Silva RG, Scheckel KG, Suidan MT, Tolaymat TM. Impact of environmental conditions (pH, ionic strength, and electrolyte type) on the surface charge and aggregation of silver nanoparticles suspensions. Environ Sci Technol 2010;44:1260–6.

Benn TM, Westerhoff P. Nanoparticle silver released into water from commercially available sock fabrics. Environ Sci Technol 2008;42:4133–9.

Blaser SA, Scheringer M, MacLeod M, Hungerbnhler K. Estimation of cumulative aquatic exposure and risk due to silver: contribution of nano-functionalized plastics and textiles. Sci Total Environ 2008;390:396–409.

Bradford A, Handy RD, Readman JW, Atfield A, Muhling M. Impact of silver nanoparticle contamination on the genetic diversity of natural bacterial assemblages in estuarine sediments. Environ Sci Technol 2009;43:4530–6.

Chappell MA, George AJ, Dontsova KM, Porter BE, Price CL, Zhou PH, et al. Surfactive stabilization of multi-walled carbon nanotube dispersions with dissolved humic substances. Environ Pollut 2009;157:1081–7.

Chemical Selection Working Group, U. S.Food & Administration Drug. Nanoscale Materials Nomination and Review of Toxicological Literature; 2006. Ref Type: Report.

Dair BJ, Saylor DM, Cargal TE, French GR, Kennedy KM, Casas RS, et al. The effect of substrate material on silver nanoparticle antimicrobial efficacy. J Nanosci Nanotechnol 2010;10:8456–62.

Elzey S, Grassian V. Agglomeration, isolation and dissolution of commercially manufactured silver nanoparticles in aqueous environments. J Nanopart Res 2010;12:1945–58.

Fauss Emma. The Silver Nanotechnology Commercial Inventory. Woodrow Wilson International Center for Scholars; 2008 http://www.nanotechproject.org/process/assets/files/6718/fauss_final.pdf.

Figueroa JAL, Wrobel K, Afton S, Caruso JA, Corona JFG, Wrobel K. Effect of some heavy metals and soil humic substances on the phytochelatin production in wild plants from silver mine areas of Guanajuato, Mexico. Chemosphere 2008;70:2084–91.

Frederix F, Friedt JM, Choi KH, Laureyn W, Campitelli A, Mondelaers D, et al. Biosensing based on light absorption of nanoscaled gold and silver particles. Anal Chem 2003;75:6894–900.

Geronimo CLA, MacCuspie RI. Antibody-mediated self-limiting self-assembly for quantitative analysis of nanoparticle surfaces by atomic force microscopy. Microsc Microanal 2011;17:206–14.

Grobelny Jaroslaw, Delrio Frank W, Pradeep Namboodiri, Kim Doo-In, Hackley Vincent A, Cook Robert F. NIST–NCL Joint Assay Protocol, PCC-6: Size Measurement of Nanoparticles Using Atomic Force Microscopy. National Institute of Standards and Technology; 2009 http://ncl.cancer.gov/working_assay-cascade.asp.

Hackley VA, Clogston JD. NIST–NCL Joint Assay Protocol PCC-1: measuring the size of nanoparticles in aqueous media using batch-mode dynamic light scattering. National Institute of Standards and Technology; 2007 http://ncl.cancer.gov/working_assay-cascade.asp.

Harper SL, Dahl JA, Maddux BLS, Tanguay RL, Hutchison JE. Proactively designing nanomaterials to enhance performance and minimise hazard. Int J Nanotechnol 2008;5:124–42.

Henig RM. Our Silver-Coated Future; 2007. p. 22–9. onearth.

Jackson AM, Hu Y, Silva PJ, Stellacci F. From homoligand- to mixed-ligand-monolayer-protected metal nanoparticles: a scanning tunneling microscopy investigation. J Am Chem Soc 2006;128:11135–49.

Lara H, Ixtepan-Turrent L, Garza T, Rodriguez-Padilla C. PVP-coated silver nanoparticles block the transmission of cell-free and cell-associated HIV-1 in human cervical culture. J Nanobiotechnol 2010;8:15.

Lee KJ, Nallathamby PD, Browning LM, Osgood CJ, Xu XHN. In vivo imaging of transport and biocompatibility of single silver nanoparticles in early development of zebrafish embryos. ACS Nano 2007;1:133–43.

Lin MY, Lindsay HM, Weitz DA, Ball RC, Klein R, Meakin P. Universality in colloid aggregation. Nature 1989;339:360–2.

Link S, El-Sayed MA. Spectral properties and relaxation dynamics of surface plasmon electronic oscillations in gold and silver nanodots and nanorods. J Phys Chem B 1999;103:8410–26.

Liu J, Hurt RH. Ion release kinetics and particle persistence in aqueous nano-silver colloids. Environ Sci Technol 2010;44:2169–75.

Liu J, Sonshine DA, Shervani S, Hurt RH. Controlled release of biologically active silver from nanosilver surfaces. ACS Nano 2010;4:6903–13.

Lok CN, Ho CM, Chen R, He QY, Yu WY, Sun H, et al. Silver nanoparticles: partial oxidation and antibacterial activities. J Biol Inorg Chem 2007;12:527–34.

Lung WS, Nice AJ. Eutrophication model for the patuxent estuary: advances in predictive capabilities. J Environ Eng-ASCE 2007;133:917–30.

Luoma SN. Silver nanotechnologies and the environment: old problems or new challenges? PEN 15, The Project on Emergine Nanotechnologies; 2008 http://www.nanotechproject.org/publications/archive/silver/.

MacCuspie RI. Colloidal stability of silver nanoparticles with various surface coatings in biologically relevant conditions. J Nanopart Res 2011, doi:10.1007/s11051-010-0178-x Early Online.

MacCuspie RI, Rogers K, Patra M, Suo Z, Allen AJ, Martin MN, Hackley VA. Challenges for comparison of physico-chemical characterization of silver nanoparticles under pristine and environmentally relevant conditions. J Environ Monit 2011b, doi:10.1039/C1EM10024F Early Online.

MacCuspie RI, Allen AJ, Hackley VA. Dispersion stabilization of silver nanoparticles in synthethetic lung fluid studied under in-situ conditions. Nanotoxicology 2011a, doi:10.3109/17435390.2010.504311 Early Online.

Malinsky MD, Kelly KL, Schatz GC, Van Duyne RP. Chain length dependence and sensing capabilities of the localized surface plasmon resonance of silver nanoparticles chemically modified with alkanethiol self-assembled monolayers. J Am Chem Soc 2001;123:1471–82.

Nallathamby PD, Lee KJ, Xu XHN. Design of stable and uniform single nanoparticle photonics for in vivo dynamics imaging of nanoenvironments of zebrafish embryonic fluids. ACS Nano 2008;2:1371–80.

Navarro E, Baun A, Behra R, Hartmann NB, Filser J, Miao AJ, et al. Environmental behavior and ecotoxicity of engineered nanoparticles to algae, plants, and fungi. Ecotoxicology 2008;17:372–86.

Oyanedel-Craver VA, Smith JA. Sustainable colloidal-silver-impregnated ceramic filter for point-of-use water treatment. Environ Sci Technol 2008;42:927–33.

Perelaer J, Hendriks CE, de Laat AWM, Schubert US. One-step inkjet printing of conductive silver tracks on polymer substrates. Nanotechnology 2009;20:165303.

Pronk MEJ, Wijnhoven Susan WP, Bleeker EAJ, Heugens Evelyn HW, Peijnenburg Willie JGM, Luttik R, et al. Nanomaterials under REACH: nanosilver as a case study. RIVM report 601780003/2009; 2009.

Ribeiro Guevara S, Arribθre M, Bubach D, Vigliano P, Rizzo A, Alonso M, et al. Silver contamination on abiotic and biotic compartments of Nahuel Huapi National Park lakes, Patagonia, Argentina. Sci Total Environ 2005;336:119–34.

Sharma VK, Yngard RA, Lin Y. Silver nanoparticles: green synthesis and their antimicrobial activities. Adv Colloid Interface Sci 2009;145:83–96.

Sondi I, Salopek-Sondi B. Silver nanoparticles as antimicrobial agent: a case study on *E. coli* as a model for Gram-negative bacteria. J Colloid Interface Sci 2004;275:177–82.

Stebounova L, Guio E, Grassian V. Silver nanoparticles in simulated biological media: a study of aggregation, sedimentation, and dissolution. J Nanopart Res 2011;13:233–44.

Templeton AC, Hostetler MJ, Kraft CT, Murray RW. Reactivity of monolayer-protected gold cluster molecules:steric effects. J Am Chem Soc 1998;120:1906–11.

Tolaymat TM, El Badawy AM, Genaidy A, Scheckel KG, Luxton TP, Suidan M. An evidence-based environmental perspective of manufactured silver nanoparticle in syntheses and applications: a systematic review and critical appraisal of peer-reviewed scientific papers. Sci Total Environ 2010;408:999-1006.

Tsai D-H, DelRio FW, Keene AM, Tyner KM, MacCuspie RI, Cho TJ, Zachariah MR, Hackley VA. Adsorption and conformation of serum albumin protein on gold nanoparticles. Langmuir 2011;27:2464–77.

Tsai D-H, DelRio FW, MacCuspie RI, Cho TJ, Zachariah M, Hackley VA. Competitive adsorption of thiolated polyethylene glycol and mercaptopropionic acid on gold nanoparticles measured by physical characterization methods. Langmuir 2010;26:10325–33.

U.S. Environmental Protection Agency. FIFRA Scientific Advisory Panel Meeting: evaluation of the hazard and exposure associated with nanosilver and other nanometal pesticide products. http://www.epa.gov/scipoly/sap/meetings/2009/november/110309ameetingminutes.pdf2010 Accessed 7-26-2010.

U.S. Food & Drug Administration. FY 2007 Regulatory Support Activities. http://www.fda.gov/AboutFDA/CentersOffices/CDRH/CDRHReports/ucm126688.htm2010 Accessed 7-26-2010.

USEPA. 821/R-02-012: Methods for measuring the acute toxicity of effluents and receiving waters to freshwater and marine organisms; 2002.
Walczyk D, Bombelli FB, Monopoli MP, Lynch I, Dawson KA. What the cell "sees" in bionanoscience. J Am Chem Soc 2010;132:5761–8.
Wen LS, Santschi PH, Gill GA, Paternostro CL, Lehman RD. Colloidal and particulate silver in river and estuarine waters of texas. Environ Sci Technol 1997;31:723–31.
Wiesner MR, Lowry GV, Jones KL, Hochella MF, Di Giulio RT, Casman E, et al. Decreasing uncertainties in assessing environmental exposure, risk, and ecological implications of nanomaterials. Environ Sci Technol 2009;43:6458–62.
Wijnhoven SWP, Peijnenburg WJGM, Herberts CA, Hagens WI, Oomen AG, Heugens EHW, et al. Nano-silver: a review of available data and knowledge gaps in human and environmental risk assessment. Nanotoxicology 2009;3:109–38.
Zook JM, MacCuspie RI, Locascio LE, Halter MD, Elliott JE. Stable nanoparticle aggregates/agglomerates of different sizes and the effect of their sizes on hemolytic cytotoxicity. Nanotoxicology 2011, doi:10.3109/17435390.2010.536615 Early Online.
Zou R, Lung WS, Wu J. Multiple-pattern parameter identification and uncertainty analysis approach for water quality modeling. Ecol Modell 2009;220:621–9.